**Title**

Disrupted segregation of working memory networks in temporal lobe epilepsy

**Permalink**

https://escholarship.org/uc/item/4jw785kj

**Authors**

Stretton, J
Winston, GP
Sidhu, M
et al.

**Publication Date**

2013

**DOI**

10.1016/j.nicl.2013.01.009

Peer reviewed

# Disrupted segregation of working memory networks in temporal lobe epilepsy ☆

J. Stretton *, G.P. Winston, M. Sidhu, S. Bonelli, M. Centeno, C. Vollmar, R.A. Cleary, E. Williams, M.R. Symms, M.J. Koepp, P.J. Thompson, J.S. Duncan

*Epilepsy Society MRI Unit, Department of Clinical and Experimental Epilepsy, UCL Institute of Neurology, Queen Square, London WC1N 3BG, UK*

## ABSTRACT

Working memory is a critical building block for almost all cognitive tasks, and impairment can cause significant disruption to daily life routines. We investigated the functional connectivity (FC) of the visuo-spatial working memory network in temporal lobe epilepsy and its relationship to the underlying white matter tracts emanating from the hippocampus. Fifty-two patients with unilateral hippocampal sclerosis (HS) (30 left) and 30 healthy controls underwent working memory functional MRI (fMRI) and Diffusion Tensor Imaging (DTI). Six seed regions were identified for FC analysis; 4 within a task-positive network (left and right middle frontal gyri and superior parietal lobes), and 2 within a task-negative network (left and right hippocampi). FC maps were created by extracting the time-series of the fMRI signal in each region in each subject and were used as regressors of interest for additional GLM fMRI analyses. Structural connectivity (SC) corresponding to areas to which the left and right hippocampi were connected was determined using tractography, and a mean FA for each hippocampal SC map was calculated. Both left and right HS groups showed atypical FC between task-positive and task-negative networks compared to controls. This was characterised by co-activation of the task-positive superior parietal lobe ipsilateral to the typically task-negative sclerosed hippocampus. Correlational analysis revealed stronger FC between superior parietal lobe and ipsilateral hippocampus, was associated with worse performance in each patient group. The SC of the hippocampus was associated with the intra-hemispheric FC of the superior parietal lobe, in that greater SC was associated with weaker parieto-frontal FC. The findings suggest that the segregation of the task-positive and task-negative FC networks supporting working memory in TLE is disrupted, and is associated with abnormal structural connectivity of the sclerosed hippocampus. Co-activation of parieto-temporal regions was associated with poorer working memory and this may be associated with working memory dysfunction in TLE.

© 2013 The Authors. Published by Elsevier Inc. All rights reserved.

## 1. Introduction

Whether the medial temporal lobe (MTL) is involved in working memory (WM) is still open to debate (Graham et al., 2010; Jeneson and Squire, 2012) but it is a fundamental question pertaining to the conceptual understanding of how memory is organised in the brain. Working memory refers to the temporary storage and manipulation of information and has typically been considered dependent on frontal lobe integrity,

independent of the MTL. Much of the evidence for this distinction relies on early studies which suggested that WM was unaffected in temporal lobe epilepsy patients (Cave and Squire, 1992; Drachman and Arbit, 1966). However, emerging evidence suggests that specific WM processes are disrupted in TLE (Abrahams et al., 1999; Krauss et al., 1997a; Owen et al., 1996) and that the MTL is involved in both short and long term memory formations (Cashdollar et al., 2009; Ranganath and Blumenfeld, 2005). Whether the disruption of WM in TLE is a result of critical MTL involvement in WM processes (Corcoran and Upton, 1993), or secondary to propagation of epileptic activity from the epileptogenic zone to eloquent cortex responsible for WM function (Hermann et al., 1988) is still unknown.

Previous imaging studies provide evidence for hippocampal involvement in specific WM processes, particularly in the context of spatial processing (Bird and Burgess, 2008) and increasing WM load (Axmacher et al., 2008). Our recent findings using a visuo-spatial WM fMRI task suggested that in TLE the ipsilateral hippocampus is unable to deactivate in response to increasing load, to the detriment of WM performance (Stretton et al., 2012). This study aimed to assess the functional connectivity patterns of the diseased hippocampus to

further understand the mechanisms of WM dysfunction in TLE. Previous studies report functionally segregated networks subserving WM; task-positive networks, involving fronto-parietal activation (Owen et al., 2005; Palacios et al., 2012) and task-negative networks, involving deactivation of the default-mode network (Palacios et al., 2012; McGill et al., 2012), including the hippocampi (Cousijn et al., 2012a). Disruption of the segregation of task-positive and task-negative networks in resting-state fMRI has been described in Idiopathic Generalised Epilepsy (IGE) (McGill et al., 2012) but has not yet been assessed in a TLE cohort.

Functional connectivity (FC) analysis of fMRI data identifies temporally correlated regions to elucidate the network dynamics for the underlying function. Several studies have investigated resting-state FC networks in TLE patients (Bettus et al., 2009a; Liao et al., 2010, 2011; Morgan et al., 2011; Waites et al., 2006) and during cognitive fMRI of WM (Axmacher et al., 2008; Campo et al., 2011), episodic memory, (Addis et al., 2007; Voets et al., 2009; Wagner et al., 2007) and language (Bonelli et al., 2012; Protzner and McAndrews, 2011; Vlooswijk et al., 2010), with mixed results. There is evidence for both increased connectivity and decreased connectivity in multiple resting state networks in TLE compared to non-TLE partial epilepsy patients (Luo et al., 2011). Furthermore, with regard to lateralization of effect, decreased ipsilateral and increased contralateral resting connectivity of the MTL epileptogenic network has been observed (Bettus et al., 2009b). In task-related connectivity studies, during complex scene encoding, the ipsilateral MTL has been shown to have reduced connectivity to the contralateral MTL and task-dependant eloquent cortex compared to controls (Voets et al., 2009). More recent work suggests that memory function in TLE may not only rely on hippocampal function alone, but also prefrontal network integrity, which shows reduced FC in cryptogenic localization-related epilepsy (Vlooswijk et al., 2011).

The underlying structure of temporal and extra-temporal white matter has also been shown to influence default mode network connectivity in TLE (Liao et al., 2011). Therefore in addition to FC, we derived a measure of structural connectivity and integrity of the white matter tracts surrounding the hippocampi. The primary measure of white matter integrity used in this study is fractional anisotropy (FA), which is determined by the directional magnitude of water diffusion in three-dimensional space. Tightly packed white matter fascicles result in water diffusion in a preferred direction (high FA), reflecting greater structural integrity. In contrast, white matter fascicles that have poor structural coherence will allow water to diffuse more randomly (low FA) reflecting white matter abnormalities. Finally, recent graph theory work suggests that the age of epilepsy onset is associated with lower temporal lobe FC, and longer duration of epilepsy is related to more random configuration of FC networks (van DE et al., 2009).

To date, no studies have investigated the segregation of task-positive and task-negative WM networks in TLE, or their relationship to the underlying structure of the temporal lobes and clinical variables such as age of epilepsy onset and seizure frequency. We hypothesised:

1) The segregation of task-positive and task-negative networks is disrupted in TLE.
2) This disruption is associated with poorer WM performance.
3) The structural connectivity of the hippocampus would influence FC network efficiency.
4) An early seizure onset and frequent seizures would be associated with greater disruption of WM networks.

## 2. Materials and methods

### 2.1. Subjects

Fifty-two patients with medically refractory TLE and unilateral hippocampal sclerosis (HS) (30 left HS, mean age 38 years, range 19–54 years; 22 right HS, mean age 41 years, range 21–56 years) undergoing pre-surgical evaluation at the National Hospital for Neurology

and Neurosurgery (NHNN) participated in this study. The study was approved by the NHNN and the Institute of Neurology Joint Research Ethics Committee, and written informed consent was obtained from all subjects.

All patients underwent structural MRI at 3 Tesla (3 T). Prolonged Video-EEG recordings confirmed seizure onset in the medial temporal lobe ipsilateral to the HS, and all patients had a normal contralateral hippocampus (volume in the range of 2.16–3.16 $mm^3$; T2 relaxation time $<118$ ms), based on qualitative and quantitative MRI criteria (Woermann et al., 1998). All patients were taking anti-epileptic drugs (AEDs), were native English speakers and had undergone a neuropsychological evaluation as part of their presurgical investigations. Clinical and demographic data are detailed in Table 1. We also recruited 30 native English speaking healthy volunteers (mean age 37 years, range 19–64 years) without any history of neurological or psychiatric disease as controls.

### 2.2. MR data acquisitions

MRI studies were performed on a 3 T GE Excite HDx scanner. Standard imaging gradients with a maximum strength of 40 mT m$^{-1}$ and slew rate 150 T m$^{-1}$ s$^{-1}$ were used. Data were acquired using an eight-channel array head coil for reception and the body coil for transmission. Gradient-echo planar T2*-weighted images were acquired, providing blood oxygenation level-dependent (BOLD) contrast. Each volume comprised 50 oblique axial 2.4 mm slices (with 0.1 mm gap) covering the whole brain, with a 24-cm field of view, SENSE factor 2, $64 \times 64$ matrix, and an in-plane resolution of $3.75 \times 3.75$ mm. Echo time (TE) was 25 ms, and repetition time (TR) was 2.5 s. Coronal T1-weighted volumetric acquisition with 170 contiguous 1.1 mm-thick slices ($256 \times 256$ matrix; in-plane resolution, $0.9375 \times 0.9375$ mm) was used for hippocampal volume measurements. The entire length of the hippocampus was measured in the coronal oblique plane on alternate slices, using a manual tracing method (Cook et al., 1992; Lemieux et al., 2000). Volumes were calculated by multiplying the sum of the cross-sectional area of each slice by the slice thickness.

**Table 1**
Clinical and demographic data.

| | Controls | Left HS | Right HS |
|---|---|---|---|
| N | 30 | 30 | 22 |
| Gender (male/female) | 12/18 | 14/16 | 5/17 |
| Handedness (right/left) | 27/3 | 26/4 | 18/4 |
| Age (years; mean; SD) | 37 (12.5) | 38 (9.8) | 41 (10.4) |
| Right HV (cm³) | 2.7 (.25) | 2.7 (.38) | 1.9 (.36)* |
| Left HV (cm³) | 2.6 (.31) | 1.7 (.36)* | 2.7 (.05) |
| Age of onset (years) | n/a | 14.5 (10.8) | 15.5 (11.9) |
| Duration of epilepsy (years) | n/a | 24 (14.1) | 26 (16.8) |
| Complex partial seizure frequency (per month) | n/a | 10.5 (16) | 6 (6.7) |
| Average no. anti-epileptic drugs (range) | n/a | 2 (1–4) | 2 (2–4) |
| Anti-epileptic drugs | n/a | LEV = 19 | LEV = 13 |
| | | CBZ = 14 | CBZ = 11 |
| | | LTG = 10 | LTG = 6 |
| | | CLB = 9 | CLB = 5 |
| | | VPA = 5 | TPM = 5 |
| | | OXC = 5 | OXC = 4 |
| | | ZNS = 4 | PHT = 3 |
| | | TPM = 3 | PGB = 3 |
| | | PGB = 1 | LCS = 2 |
| | | | PB = 2 |
| | | | ZNS = 1 |
| | | | PRM = 1 |

HS = Hippocampal Sclerosis; HV = Hippocampal Volume; * = Significant at $p<0.05$ following one-way ANOVA; CBZ = Carbamazepine; LEV = Levetiracetam; VPA = Sodium Valproate; LTG = Lamotrogine; LCS = Lacosimide; TPM = Topiramate; PHT = Phenytoin; ZNS = Zonisimide; CLB = Clobazam; OXC = Oxcarbazepine; PGB = Pregabalin; PB = Phenobarbitone; PRM = Primidone.

### 2.3. Diffusion Tensor Imaging (DTI) acquisition

In 6 of the 82 participants, (3 controls, 2 left HS and 1 right HS) DTI acquisition failed due to technical difficulties (loss of pulse rate monitor). Data were acquired using a cardiac-triggered single-shot spin-echo planar imaging sequence with echo time = 73ms. Sets of 60 contiguous 2.4 mm-thick axial slices were obtained covering the whole brain, with diffusion sensitizing gradients applied in each of 52 non-collinear directions ($b$ value of 1200 mm$^2$ s$^{-1}$ [δ = 21 ms], Δ = 29 ms using full gradient strength of 40 mT m$^{-1}$) along with 6 non-diffusion weighted scans. Gradient directions were calculated and ordered as described elsewhere (Cook et al., 2007). Field of view was 24 cm, with matrix size of 96 × 96, zero filled to 128 × 128 during reconstruction, giving a reconstructed voxel size of 1.875 mm × 1.875 mm × 2.4 mm. The first four scans were discarded to ensure magnetization equilibrium.

### 2.4. 'Dot-Back' fMRI paradigm

Subjects were required to monitor the locations of dots (presentation time: 440 ms; inter-stimulus interval: 1500 ms) within a diamond shaped box on the screen at a given delay from the original occurrence (0-, 1-, or 2-back). There were three 30-s active conditions in total (0-, 1-, and 2-back) presented to subjects five times in pseudorandom order, controlling for any order effect. In total, 15 stimuli were presented in each 30-s active block. Each active condition started with a 15-s resting baseline (the word 'Rest' appeared on the screen during this period). Subjects were required to move the joystick corresponding to the correct location of the current (0-back) dot, the location of the previously presented dot (1-back) or the location of the dot appearing two presentations before (2-back).

### 2.5. Data analysis

Imaging data were analysed with Statistical Parametric Mapping (SPM8) (www.fil.ion.ucl.ac.uk). The time series of each subject was realigned, spatially normalized to an acquisition-specific echo planar imaging template in Montreal Neurological Institute space, and smoothed with a Gaussian kernel of 8 mm full-width at half maximum. Trial-specific responses were modelled by convolving a delta function that indicated each block onset with the canonical hemodynamic response function to create regressors of interest. Each subject's movement parameters were included as confounds. Contrasts were defined to identify task-positive areas comparing high memory load ('2-back') against the control task ('0-back'). To identify task-negative areas, i.e. areas progressively deactivated with increasing task difficulty, we defined an additional contrast with values −1, −2 and −3 for the three conditions '0-back', '1-back' and '2-back', modelling such deactivation compared with the resting periods. These contrast images were subsequently used to define seed regions for the FC analysis.

### 2.6. Functional connectivity analysis

Based on established working memory network nodes (Owen et al., 2005), four regions of interest (ROIs) were defined from the task-positive contrast; left and right middle frontal gyri (MFG), left and right superior parietal lobes (SPL). Based on our previous finding of disrupted hippocampal deactivation in TLE during the task (Stretton et al., 2012), two ROIs were defined using the task-negative contrast in the left and right medial temporal lobes (MTL) (Fig. 1). ROIs were defined using a combination of functional and anatomical criteria: clusters revealed by the combined group (left HS, right HS and controls) and main effect of task (thresholded at p<0.05 FWE) of the respective regions were inclusively masked with the corresponding anatomical regions of interest (ROI) of the WFU Pick Atlas toolbox (Tzourio-Mazoyer et al., 2007; Maldjian et al., 2003). Regional time series were extracted from each ROI on the single-subject level. The average time series from the peak voxel within all six ROIs for each individual were used as regressors for new general linear model fMRI analyses. These individual first level contrast images were then taken to the second-level for group analysis for each seed region.

Analysis of variance (ANOVA) was performed with group as a factor to examine the main effects of each connectivity seed ROI and to highlight regions demonstrating more or less FC in one group compared to another. We report all activations at a threshold of p<0.001, uncorrected for multiple comparisons, if not stated otherwise. In view of our a priori hypothesis we performed small volume corrections (SVC) on results indicating activation within the hippocampus, defined as a 6 mm sphere surrounding the peak voxel in the cluster. This was adopted as we were testing a specific hypothesis regarding MTL activity and because of the low signal-to-noise ratio in the anterior temporal lobe.

### 2.7. Independent component analysis

In order to identify the task specificity of the functional connectivity maps, independent component analysis was carried out at a group level using MELODIC from FMRIB software library (http://www.fmrib.ox.ac.uk/fsl/) (Beckmann and Smith, 2005). A 4D file of the realigned, normalized, smoothed images was created for each subject, and image data were prefiltered with a high-pass filter with a cut-off at 100 s. The algorithm was constrained to identify 32 independent components, common across all subjects in each group and characterised with regard to their location, spatial extent and signal time course. Components were ranked according to their relative contribution to overall signal variance, and no manual selection or rejection of components was carried out (Vollmar et al., 2011).

### 2.8. Structural connectivity

Eddy current correction of the DTI data was performed using the eddy correct tool in FSL (version 4.0.1) (Smith et al., 2004) and the Camino toolkit (version 2, release 767) was used to calculate fractional anisotropy (FA) images for each subject. Automated segmentation of the T1-weighted volumetric scans using Freesurfer was used to identify the hippocampi (http://surfer.nmr.mgh.harvard.edu/). The b = 0 image from the DTI scan was affinely registered to the T1 volumetric scan using FLIRT (http://www.fmrib.ox.ac.uk/fsl/flirt/index.html). The inverse transformation was applied to the segmentation to give the hippocampal seeds in native diffusion space. Tractography was performed from the hippocampal seeds employing a multi-tensor model with 1000 iterations from each voxel within the seed region as previously described (Winston et al., 2012). The connectivity distributions generated for each subject were thresholded at 0.05 and the mean FA of the areas to which each hippocampus was connected was determined to give a global measure of hippocampal structural connectivity used for subsequent analyses (Fig. 1). Greater mean FA was interpreted as a measure of greater structural connectivity of the hippocampus.

### 2.9. Neuropsychological assessment

#### 2.9.1. Digit span backwards

The Digit span subtest from the WAIS-R (Wechsler, 1981) was administered to each participant and the digit span backwards trials were used as the measure of WM. The participants have to repeat digit strings of increasing length in the reverse order. Digit sequences ranged from 2 to 8 with two trials per sequence. Span size was calculated as the highest digit sequence where both trials were successful (max score = 8).

#### 2.9.2. Gesture span

The gesture span task (Canavan et al., 1989) requires the subject to copy sequences of hand gestures of increasing length up to 5 gestures. The test ends when participants make two consecutive errors
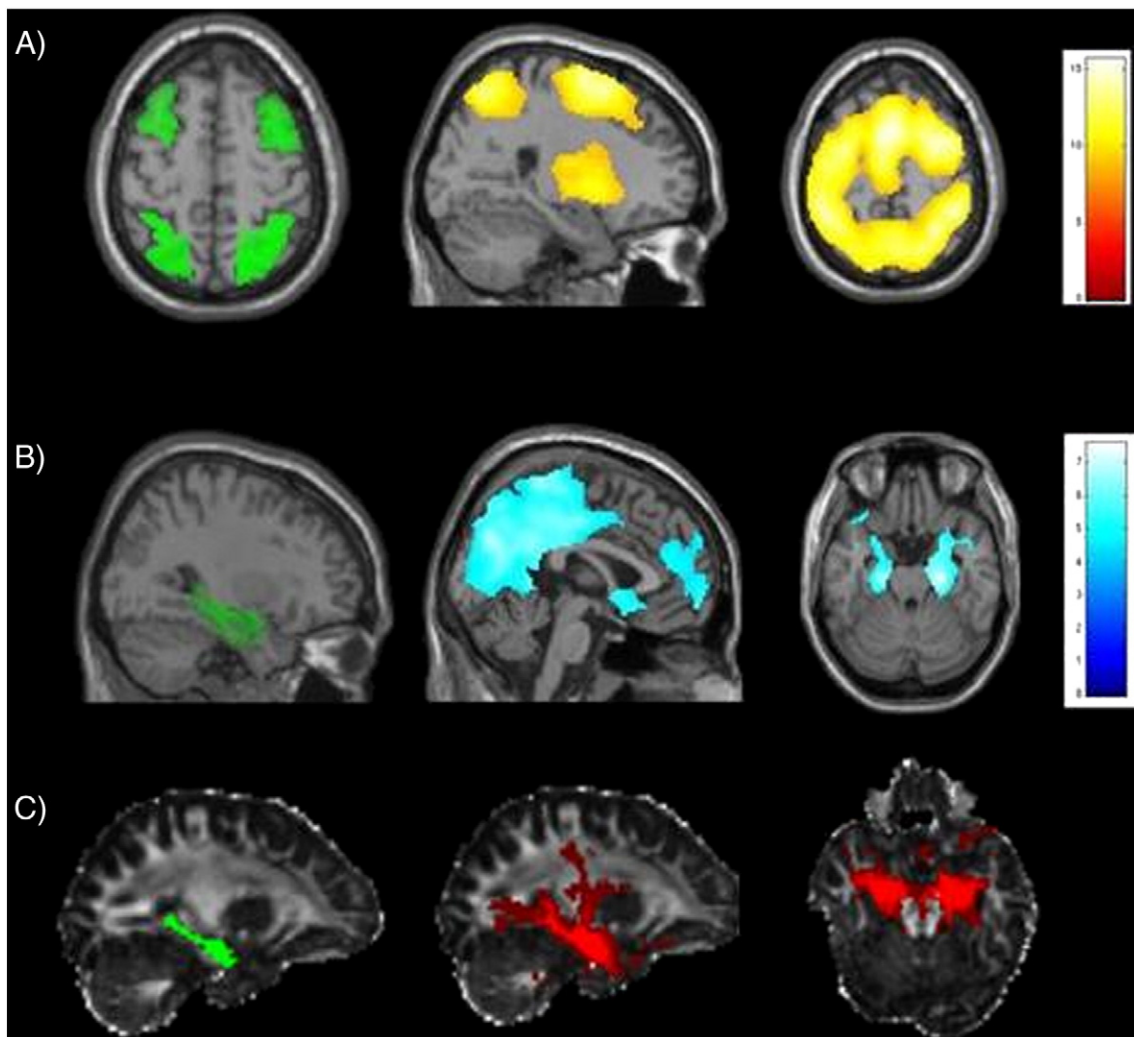
**Fig. 1.** Functional and structural connectivity seed regions and maps. A. Task-positive seed regions of the bilateral middle frontal gyri and superior parietal lobes (green, axial slice) and control group FC maps showing co-activation of a fronto-thalamo-parietal network between each region (yellow). B. Task-negative seed region of the medial temporal lobe (green, sagittal slice) and control group FC map showing co-deactivation of default mode network regions and bilateral hippocampus (blue). Images are overlaid on a single-subject T1 image provided by SPM8. C. Structural connectivity (SC) seed regions of the hippocampus (green, sagittal slice) and individual control SC map showing areas connected to each hippocampus (red). The mean fractional anisotropy (FA) value was calculated in each subject for each hippocampal SC map and used for subsequent analyses. Images are overlaid on a control subject FA image.

at any given gesture set size or when the maximum of 5 gestures had been reached. The task was repeated with a parallel version immediately after the first version was finished. One point was given for each successful trial. The mean span was calculated across trials and was used for the subsequent analysis (max score = 5).

### 2.9.3. Motor sequences

The motor sequence task devised by Canavan (Canavan et al., 1989) requires a sequence of 3 hand gestures to be repeated in the same order. Ten alternating sequences were administered in total. The test stopped after all 10 trials had been completed. One point was given for each successful trial. The total number of successful trials was used for the subsequent analysis (max score = 10).

### 2.9.4. Working memory: composite score

In order to explore the relationship between WM competence and neural activation patterns, and to avoid multiple comparisons, a single measure of WM was derived using a principal component analysis (PCA). Out of scanner scores for digit backwards, gesture span, and motor sequences as well as performance from the most demanding 2-back fMRI condition were entered into a PCA. The derived score for each subject was then entered as a regressor of interest into an analysis

of covariance (ANCOVA) in order to test for correlations between areas of FC and performance. Neuropsychological data were analysed using PASW-v18 (SPSS; Chicago, IL, USA).

## 3. Results

### 3.1. Working memory performance

One-way ANOVA revealed that both left HS and right HS groups performed significantly less well than controls in all working memory measures (p < 0.05) apart from the right HS group in the 2 dot-back condition of the fMRI task (p = 0.08). Similarly, the composite working memory score derived from the PCA was significantly lower in patients than controls (p < 0.001) (Table 2).

### 3.2. Functional connectivity group maps

Seeding from the left and right MFG and SPL, each group showed co-activation within a fronto-thalamo-parietal network of task-positive regions. Seeding from the left and right MTL, each group showed co-deactivation with the contralateral MTL, lateral temporal lobes and

**Table 2**
Neuropsychological data (mean and standard deviations).

| Group (n) | Digit Span backwards (/8) | Gesture span (/6) | Motor sequences (/10) | 2 dot back % | Principal component |
|---|---|---|---|---|---|
| Controls (30) | 4.7 (1.1) | 3.2 (.6) | 6.4 (1.9) | 70 (20) | .67 (.86) |
| Left HS (30) | 3.6 (1.1)* | 2.5 (.7)* | 4.2 (1.9)* | 51 (22.9)* | −.48 (.84)* |
| Right HS (22) | 3.3 (.9)* | 2.6 (.8)* | 4.1 (2.3)* | 56 (22.9) | −.40 (.91)* |

HS = Hippocampal Sclerosis; * = One-way ANOVA results, significant p<0.05 compared to controls.

default mode regions including the precuneus, anterior cingulate cortex (ACC) and medial frontal gyrus (Fig. 1).

### 3.3. Functional connectivity group differences

There was no significant reduction in connectivity for any of the six seed regions in the left and right HS groups compared to controls but increased connectivity was observed (see Table 3).

#### 3.3.1. Middle frontal gyri
The left HS group showed increased co-activation of the left MFG, with the left hippocampus (−20, −10, −14, p<0.05 FWE SVC) (Fig. 2). The right HS group showed increased co-activation of the left MFG with the right ACC (Cashdollar et al., 2009; Bonelli et al., 2012; Palacios et al., 2012).

#### 3.3.2. Superior parietal lobes
The left HS group showed increased co-activation of the left and right SPL, with the left hippocampus (−36, −18, −16, p<0.05 FWE SVC). In the right HS group, the right SPL had increased co-activation with the right hippocampus (36, −12, −20, p<0.05 SVC) (Fig. 2).

#### 3.3.3. Medial temporal lobes
For both the left and right MTL seed regions, both left and right HS groups showed increased contralateral MTL co-deactivation compared to controls (p<0.05 FWE SVC).

### 3.4. Independent component analysis

The 32 independent components identified by independent component analysis described 87% of the total functional MRI signal variance in controls, 80% in left HS and 82% in right HS. In controls, the first component (explaining 6% of the total signal variance) was located in the bilateral MFG, left central region, bilateral SPL and anti-correlation of the precuneus, representing the working memory network, motor response and the default mode network respectively.. This component's signal changes were time-locked to the task timing (frequency 1/45 s), and the response showed a strong correlation with the cognitive load from the task, with higher amplitude in more difficult conditions (Fig. 3A). A similar component was identified in the right HS group (explaining 7.7% of total variance) but was less well modulated by task difficulty (Fig. 3B). In the left HS group, a disproportionately large component (explaining 35.6% of the total variance) compromising the bilateral MFG, left central region and to a lesser extent bilateral SPL represented a less extensive working memory network with no evidence of anti-correlation with the default mode network (Fig. 3C). This could represent a ceiling effect in the left HS group reflected by the relatively equal amplitude across all three conditions.

### 3.5. Regression analyses

#### 3.5.1. WM performance

*3.5.1.1. Middle frontal gyri.* In controls, greater WM performance was associated with co-activation of the contralateral MFG for both left and right seeds. Poorer performance was associated with co-activation of the precuneus for both left and right MFG seeds (Fig. 4). There was no correlation with performance in either the left or right HS groups for either MFG seed region.

*3.5.1.2. Superior parietal lobes.* Co-activation of the left and right SPL with the precuneus was associated with poorer performance in the control group. In the left HS group, poorer performance was associated with increased co-activation of the left hippocampus with the left SPL, and of both hippocampi with the right SPL. In the right HS group, poorer performance was associated with co-activation of the right SPL and right parahippocampal gyrus (Fig. 4).
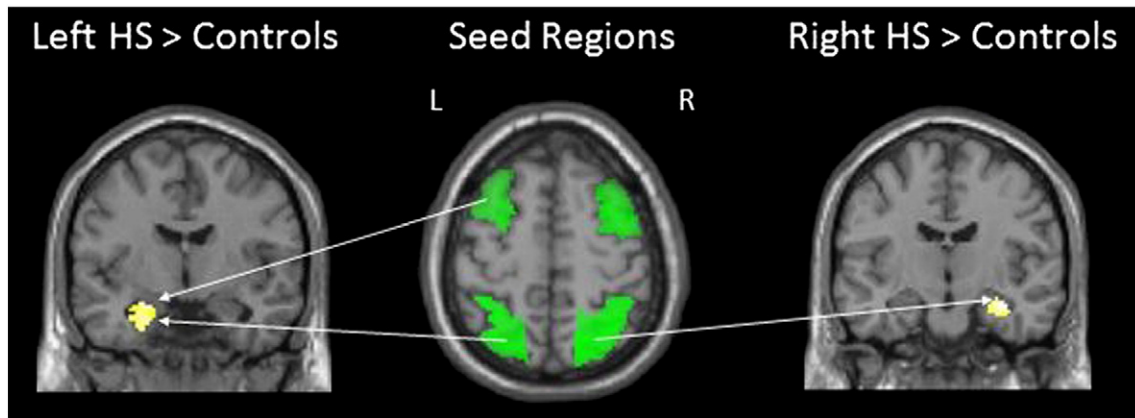
**Table 3**
fMRI peak activation group differences for each FC seed region.

| Seed region | Group/interaction | Z-score | p-value | Peak coordinates (x, y, z) in MNI space | Anatomical region |
|---|---|---|---|---|---|
| Left MFG | Left HS>Controls | **3.89** | **0.001** | **− 56, 22, 20** | **L. inferior frontal gyrus** |
| | | 3.83 | 0.001 | −10, −2, 50 | L. suppl. motor area |
| | | 3.24 | 0.05* | −20, −10, −14 | L. hippocampus |
| | Right HS>Controls | **3.79** | **0.001** | **8, 28, 16** | **R. ant. cingulate cortex** |
| Right MFG | Left HS>Controls | – | – | – | – |
| | Right HS>Controls | – | – | – | – |
| Left SPL | Left HS>Controls | **3.81** | **0.001** | **− 40, − 22, 20** | **L. insula** |
| | | 3.59 | 0.001 | −22, −2, −20 | L. amygdala |
| | | 3.16 | 0.05* | −36, −18, −16 | L. hippocampus |
| | Right HS>Controls | – | – | – | – |
| Right SPL | Left HS>Controls | **2.93** | **0.05*** | **− 36, − 18, − 16** | **L. hippocampus** |
| | Right HS>Controls | **2.31** | **0.05*** | **36, − 12, − 20** | **R. hippocampus** |
| Left hippocampus | Left HS>Controls | **4.50** | **0.05 FWE** | **44, − 76, 40** | **R. inferior parietal lobe** |
| | | 3.77 | 0.001 | −18, −82, 52 | R. superior parietal lobe |
| | | 3.58 | 0.001 | −24, −8, −20 | L. hippocampus |
| | | 3.52 | 0.001 | 18, −4, −22 | R. hippocampus |
| | Right HS>Controls | – | – | – | – |
| Right hippocampus | Left HS>Controls | **3.81** | **0.001** | **− 22, − 28, − 4** | **L. hippocampus** |
| | | 3.66 | 0.001 | 22, −4, −20 | R. hippocampus |
| | Right HS>Controls | 3.60 | 0.001 | −30, −22, −12 | L. hippocampus |

FWE = Family-Wise Error corrected; MFG = Middle Frontal Gyrus; SPL = Superior Parietal Lobe; HS = Hippocampal Sclerosis; MNI = Montreal Neurological Institute; L = left; R = right. Results highlighted in bold represent the global maxima. Results with a '–' indicates no significant voxels.
* p<0.05 Family-Wise Error corrected after small volume correction using a 6 mm sphere.

**Fig. 2.** Functional connectivity group differences. Compared to controls, left HS patients showed greater co-activation of the left superior parietal lobe (SPL) and left middle frontal gyrus (MFG) with the left hippocampus, while right HS patients showed greater co-activation of the right SPL and right hippocampus. HS = Hippocampal Sclerosis; L = Left; R = Right. Images are overlaid on a single-subject T1 image provided by SPM8.

*3.5.1.3. Medial temporal lobes.* There was no significant correlation with performance in any group with either the left or right MTL seed regions.

*3.5.2. Structural connectivity*

One-way ANOVA revealed left HS patients to have significantly lower FA values in both the left ($p<0.0001$) and right ($p<0.01$) hippocampal SC maps compared to controls. Right HS patients showed reduced FA only in the right hippocampus SC map ($p<0.005$).

Inline Supplementary Table S1 can be found online at http://dx.doi.org/10.1016/j.nicl.2013.01.009.

In all three groups, the FA of the left and right hippocampus SC maps correlated with FC from the SPL seeds, but not with the MFG seeds.

In controls, lower right hippocampal SC was associated with co-activation of the right SPL and right inferior frontal gyrus. Lower left hippocampal SC was associated with greater co-activation of the left SPL and bilateral MFG ($p<0.01$ uncorrected).

In the left HS group, lower left hippocampal SC was associated with co-activation of the left SPL and the (task-negative) left medial frontal gyrus ($p<0.01$ uncorrected). However, unlike controls, greater SC of the right hippocampus was associated with greater co-activation of the right SPL and right MFG.

In the right HS group, lower right hippocampal SC was associated with co-activation of the right SPL and the (task-negative) bilateral medial frontal gyrus. Similar to controls, lower left hippocampal SC was associated with co-activation of the left SPL and the left superior frontal gyrus.

*3.6. Correlation with clinical variables*

In the left HS group, younger age of onset was associated with increased co-activation of the task-negative left MTL and task-positive right MFG. In addition, greater seizure frequency was associated with co-activation of the task-negative left MTL and task-positive left inferior frontal gyrus in the left HS group. There was no significant correlation with hippocampal volume in any group for any seed region.

## 4. Discussion

### 4.1. Summary of main findings

In TLE there was a disrupted segregation of task-positive and task-negative networks, and this was associated with poorer WM. In addition, the SC of the hippocampus was associated with the FC of the parietal seed regions.
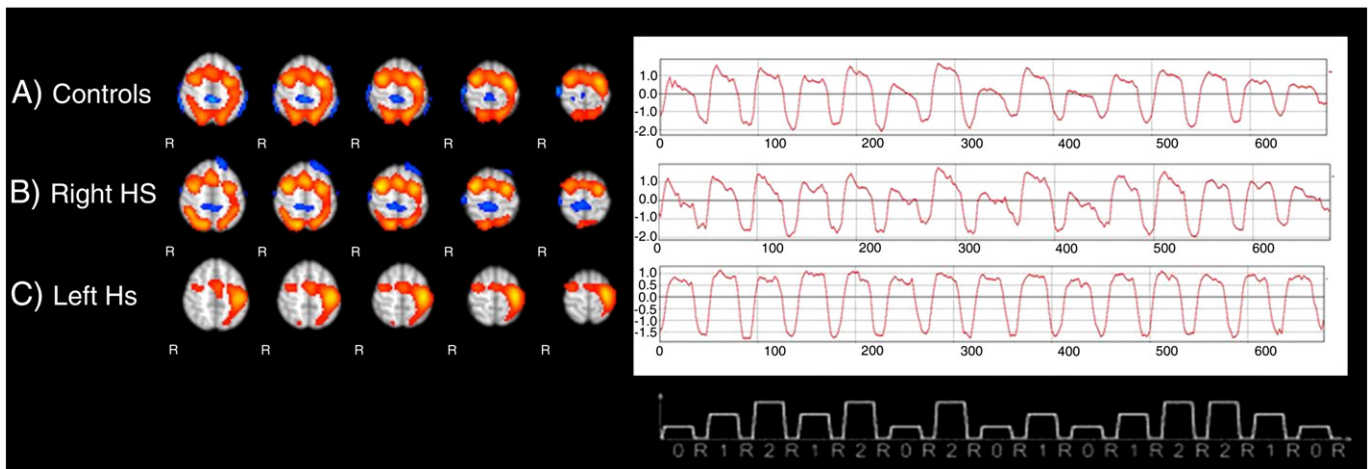


**Fig. 3.** Independent component analysis results. The first component of the controls (A) shows task-modulated fronto-parietal network connections with anti-correlation of the precuneus. The right HS group (B) follow a similar pattern but with less modulatory effect of the task. The left HS group (C) first component compromised the bilateral MFG, left central region and to a lesser extent bilateral SPL modulated equally by each condition. HS = Hippocampal Sclerosis.
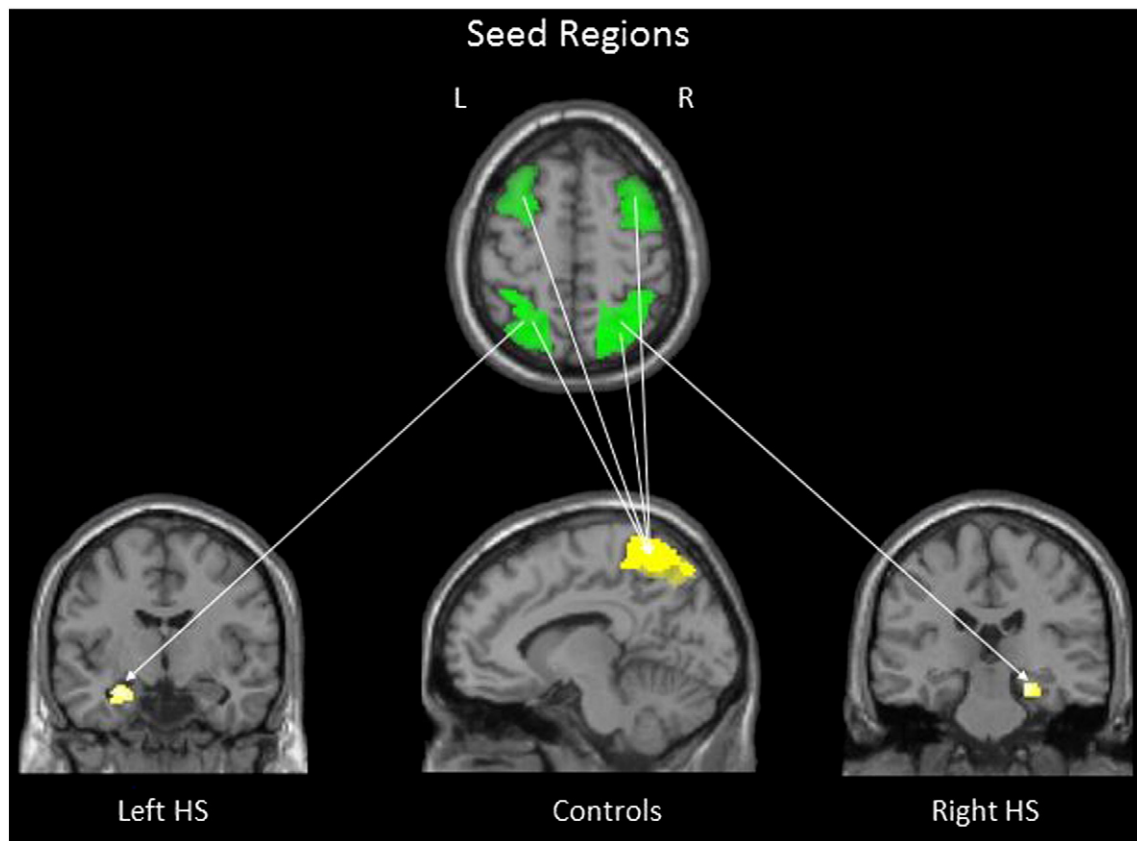
**Fig. 4.** Functional connectivity; correlation with working memory performance. Co-activation of the left SPL and left hippocampus, and right SPL with the right parahippocampal gyrus, was associated with poor performance in the left and right HS groups respectively. In controls, there was co-activation of the task-positive seeds with the task-negative precuneus. HS = Hippocampal Sclerosis; L = Left; R = Right. Images are overlaid on a single-subject T1 image.

### 4.2. Comparison with previous literature

Both left and right HS patients performed less well than controls across all measures of WM. This is in keeping with other evidence suggesting WM impairments in TLE (Abrahams et al., 1999; Owen et al., 2005; Axmacher et al., 2007; Black et al., 2010; Grippo et al., 1996; Krauss et al., 1997b; Wagner et al., 2009) implying a critical role for the hippocampus in WM functions. Previous connectivity studies of WM in TLE reinforce these findings. In a recent study, Campo and colleagues (Campo et al., 2011) compared dynamic causal models extracted from MEG recordings during verbal WM encoding in 11 left HS patients and 11 healthy volunteers. The controls performed significantly better than the left HS group and model comparison revealed a bilateral bi-directional model including frontal and temporal nodes yielded the most convincing representation of verbal WM. Comparing this model between groups, the left HS patients showed a reduced ipsilateral backward connection from the left hippocampus to the left inferior temporal cortex. Contralaterally, patients showed significantly increased forward connections from the right hippocampus to the right inferior frontal gyrus (IFG) compared to controls, and backward connections from the right IFG and right hippocampus which were associated with poorer performance (Campo et al., 2011). Our results add to this evidence, suggesting that the FC networks subserving WM in TLE are disrupted both local to and remote from the epileptogenic zone.

We identified two networks associated with the WM fMRI task. One network comprised the task-positive regions typically associated with WM, namely the MFG and SPL. The fronto-parietal task-positive network relates to the short-term storage and manipulation of information needed for goal-orientated behaviour that underpins WM processes. The other task-negative network comprised areas of the default mode network (DMN) that deactivate during cognitive effort (Raichle et al., 2001), including the hippocampi. Deactivation of the hippocampus during WM has previously been observed in schizophrenia (Meyer-Lindenberg et al., 2001) and healthy volunteers (Astur and Constable, 2004; Astur et al., 2005; Cousijn et al., 2012b; Hampson et al., 2006). In controls, these networks were functionally segregated, in line with previous evidence (Fair et al., 2007). Both left and right HS groups, however, showed disrupted segregation of the task-positive and task-negative networks, with greater ipsilateral co-activation of the SPL and MTL relative to controls. Disrupted segregation of task-positive and task-negative networks has been reported in traumatic brain injury (Palacios et al., 2012), autism (Rudie et al., 2012) and other epilepsy syndromes (McGill et al., 2012; Vollmar et al., 2011).

Using the same fMRI paradigm, patients with Juvenile Myoclonic Epilepsy (JME) have shown increased co-activation of the motor cortex and the fronto-parietal network as task demands increase. Moreover, the default mode regions remained relatively more active during the task compared to controls (Vollmar et al., 2011). In IGE, using resting-state fMRI, default mode network abnormalities were observed showing co-activation between positive-frontal and negative-parietal regions compared to controls (McGill et al., 2012).

Our study underlines the importance of network segregation utilising task-related FC. WM performance negatively correlated with co-activation of the task-positive seeds and the task-negative region of the precuneus in controls. In TLE, co-activation of ipsilateral parieto-temporal regions was associated with poorer WM, suggesting that dysfunction of the sclerotic hippocampus may impair the segregation of WM networks in these patients. The group ICA revealed task-specific WM network components in our controls and right HS group and to a lesser extent in the left HS group. In the left HS group,

the first component explained almost 36% of the total signal variance, reflecting the heterogeneity of connectivity within the left HS group. While this could influence the interpretation of the FC results, perhaps reflecting reduced task compliance, it is noted that there was no significant difference in task performance between the left and right HS groups. Furthermore, the ipsilateral parieto-temporal increases and related correlations with poor performance are also seen in the right HS group. However, it is of note that there was no correlation between medial temporal lobe FC and performance in any group, only from the task-positive superior parietal lobe. Further measures of effective connectivity to infer causality and direction of effect would be needed to explore this result. Finally, in the left HS group younger age of onset and more frequent seizures were associated with more marked disruption of networks. This is in keeping with findings that earlier insult and higher seizure frequency are more disruptive to functional network architecture (Janszky et al., 2003; Kaaden et al., 2011).

Thus, evidence from both the generalised and focal (TLE) epilepsy studies indicate that disrupted segregation of functional networks could be a common phenomenon of epilepsy, with syndrome-specific effects depending on the epileptogenic networks involved in each syndrome.

We also report a novel observation that the SC of the hippocampus, independent of task, is associated with the segregation of FC networks. The SC of the hippocampus was not associated with connectivity of the frontal lobe seeds and only showed a relationship with the parietal seed regions. Lower FA values of the left and right hippocampus SC maps were associated with greater ipsilateral parieto-frontal connectivity in our control group. Interestingly, in the left HS group we observed an opposite effect in the contralateral hippocampus, where greater FA of the right hippocampus SC map was associated with increased right-sided parieto-frontal connectivity. This could be interpreted as structural compensation of the contralateral hippocampus which has previously been reported at a functional level during verbal WM (Campo et al., 2011). In keeping with previous evidence, the FA of the ipsilateral hippocampus SC map in both patient groups was significantly lower than controls (Focke et al., 2008). However in patients lower FA of the ipsilateral hippocampus SC map was associated with co-activation of the ipsilateral task-positive SPL with task-negative DMN, again implying weaker segregation of WM networks with more severe pathology.

White matter integrity has previously been shown to influence resting-state FC in TLE (Liao et al., 2010) and extra-temporal regions, including the parietal lobe have been shown to be atrophied in TLE (Riley et al., 2010; Keller and Roberts, 2008), suggesting that white matter degradation associated with chronic uncontrolled seizure can disrupt the functional connectivity of regions local to and remote from the epileptogenic temporal lobe. These results taken together with our findings suggest that the temporo-parietal connectivity network may be as much at risk in drug-resistant TLE as frontal lobe networks.

### 4.3. Strengths and limitations

A major strength of our study is the large homogenous group of HS patients. Using patients with unilateral pathology in a bilateral task allowed us to identify laterality effects regarding the ipsilateral architecture of WM networks in relation to hippocampal pathology. Assessing functional connectivity derived from an average time series across a cognitive task as opposed to resting state data can limit the interpretation of the results. As our block design includes three 'active' conditions and resting periods the observed correlations may be driven, for example, by the rest condition and not by the task itself. However, the ICA identified task modulated functional connectivity networks involving the task-positive nodes we used. To understand the direction of effects, methods assessing effective connectivity such as dynamic causal modelling or psycho-physiological interactions could infer the causal influence between seeds that would facilitate our understanding of the neural networks supporting WM. Both patient

groups performed significantly less well on the motor sequence task and gesture span task than the controls, which could have impacted on the ability to manoeuvre the in-scanner joystick. However the joystick response inside the scanner is equivalent to a gesture span of one, and this level of ability was reached by each participant in this study therefore it is unlikely that these results impacted on the use of the joystick. It is also important to note that although we have found similar results to those in other epilepsy syndromes regarding the segregation of positive and negative networks, there are distinct methodological differences between these studies regarding the use of resting-state versus task-based connectivity measures. The impact of AEDs on FC is yet to be determined, and may significantly confound our results. The effect of Topiramate on cognition is well documented (Szaflarski and Allendorfer, 2012) and it has recently been shown that lamotrigine can inhibit the effective connectivity of motor circuits and increase the connectivity of prefrontal circuitry (Li et al., 2011).

## 5. Conclusion

We identified disrupted segregation of the task-positive and task-negative networks supporting the critical cognitive function of working memory in TLE with HS. Co-activation of ipsilateral parieto-temporal regions was associated with poorer performance in both left and right HS patients and this may be associated with WM dysfunction in TLE. This study supports the notion of hippocampal dependent working memory and provides further evidence of remote effects associated with drug-resistant TLE from both functional and structural perspectives. Further work is needed to identify the causal influence of this disruption and whether this effect is specific to working memory or reproducible with other cognitive fMRI paradigms. Finally it will be essential to evaluate the impact of temporal lobe surgery on the functional segregation of cognitive networks.

## References

Graham, K.S., Barense, M.D., Lee, A.C., 2010. Going beyond LTM in the MTL: a synthesis of neuropsychological and neuroimaging findings on the role of the medial temporal lobe in memory and perception. Neuropsychologia 48, 831–853 (Mar).

Jeneson, A., Squire, L.R., 2012. Working memory, long-term memory, and medial temporal lobe function. Learning and Memory 19, 15–25 (Jan).

Cave, C.B., Squire, L.R., 1992. Intact verbal and nonverbal short-term memory following damage to the human hippocampus. Hippocampus 2, 151–163 (Apr).

Drachman, D.A., Arbit, J., 1966. Memory and the hippocampal complex. II. Is memory a multiple process? Archives of Neurology 15, 52–61 (Jul).

Abrahams, S., Morris, R.G., Polkey, C.E., et al., 1999. Hippocampal involvement in spatial and working memory: a structural MRI analysis of patients with unilateral mesial temporal lobe sclerosis. Brain and Cognition 41, 39–65 (Oct).

Krauss, G.L., Summerfield, M., Brandt, J., Breiter, S., Ruchkin, D., 1997a. Mesial temporal spikes interfere with working memory. Neurology 49, 975–980 (Oct).

Owen, A.M., Morris, R.G., Sahakian, B.J., Polkey, C.E., Robbins, T.W., 1996. Double dissociations of memory and executive functions in working memory tasks following frontal lobe excisions, temporal lobe excisions or amygdalo-hippocampectomy in man. Brain 119 (Pt 5), 1597–1615 (Oct).

Cashdollar, N., Malecki, U., Rugg-Gunn, F.J., Duncan, J.S., Lavie, N., Duzel, E., 2009. Hippocampus-dependent and -independent theta-networks of active maintenance. Proceedings of the National Academy of Sciences of the United States of America 106, 20493–20498 (Dec 1).

Ranganath, C., Blumenfeld, R.S., 2005. Doubts about double dissociations between short- and long-term memory. Trends in Cognitive Sciences 9, 374–380 (Aug).

Corcoran, R., Upton, D., 1993. A role for the hippocampus in card sorting? Cortex 29, 293–304 (Jun).

Hermann, B.P., Wyler, A.R., Richey, E.T., 1988. Wisconsin Card Sorting Test performance in patients with complex partial seizures of temporal-lobe origin. Journal of Clinical and Experimental Neuropsychology 10, 467–476 (Aug).

Bird, C.M., Burgess, N., 2008. The hippocampus and memory: insights from spatial processing. Nature Reviews Neuroscience 9, 182–194 (Mar).

Axmacher, N., Schmitz, D.P., Wagner, T., Elger, C.E., Fell, J., 2008. Interactions between medial temporal lobe, prefrontal cortex, and inferior temporal regions during visual working memory: a combined intracranial EEG and functional magnetic resonance imaging study. Journal of Neuroscience 28, 7304–7312 (Jul 16).

Stretton, J., Winston, G., Sidhu, M., et al., 2012. Neural correlates of working memory in temporal lobe epilepsy—an fMRI study. NeuroImage 60, 1696–1703 (Apr 15).

Owen, A.M., McMillan, K.M., Laird, A.R., Bullmore, E., 2005. N-back working memory paradigm: a meta-analysis of normative functional neuroimaging studies. Human Brain Mapping 25, 46–59 (May).

Palacios, E.M., Sala-Llonch, R., Junque, C., et al., 2012. White matter integrity related to functional working memory networks in traumatic brain injury. Neurology 78, 852–860 (Mar 20).

McGill, M.L., Devinsky, O., Kelly, C., et al., 2012. Default mode network abnormalities in idiopathic generalized epilepsy. Epilepsy & Behavior 23, 353–359 (Mar).

Cousijn, H., Rijpkema, M., Qin, S., van Wingen, G.A., Fernandez, G., 2012a. Phasic deactivation of the medial temporal lobe enables working memory processing under stress. NeuroImage 59, 1161–1167 (Jan 16).

Bettus, G., Guedj, E., Joyeux, F., et al., 2009a. Decreased basal fMRI functional connectivity in epileptogenic networks and contralateral compensatory mechanisms. Human Brain Mapping 30, 1580–1591 (May).

Liao, W., Zhang, Z., Pan, Z., et al., 2010. Altered functional connectivity and small-world in mesial temporal lobe epilepsy. PLoS One 5, e8525.

Liao, W., Zhang, Z., Pan, Z., et al., 2011. Default mode network abnormalities in mesial temporal lobe epilepsy: a study combining fMRI and DTI. Human Brain Mapping 32, 883–895 (Jun).

Morgan, V.L., Rogers, B.P., Sonmezturk, H.H., Gore, J.C., Abou-Khalil, B., 2011. Cross hippocampal influence in mesial temporal lobe epilepsy measured with high temporal resolution functional magnetic resonance imaging. Epilepsia 52, 1741–1749 (Sep).

Waites, A.B., Briellmann, R.S., Saling, M.M., Abbott, D.F., Jackson, G.D., 2006. Functional connectivity networks are disrupted in left temporal lobe epilepsy. Annals of Neurology 59, 335–343 (Feb).

Campo, P., Garrido, M.I., Moran, R.J., et al., 2011. Remote effects of hippocampal sclerosis on effective connectivity during working memory encoding: a case of connectional diaschisis? Cerebral Cortex (Aug 1).

Addis, D.R., Moscovitch, M., McAndrews, M.P., 2007. Consequences of hippocampal damage across the autobiographical memory network in left temporal lobe epilepsy. Brain 130, 2327–2342 (Sep).

Voets, N.L., Adcock, J.E., Stacey, R., et al., 2009. Functional and structural changes in the memory network associated with left temporal lobe epilepsy. Human Brain Mapping 30, 4070–4081 (Dec).

Wagner, K., Frings, L., Halsband, U., et al., 2007. Hippocampal functional connectivity reflects verbal episodic memory network integrity. Neuroreport 18, 1719–1723 (Oct 29).

Bonelli, S.B., Thompson, P.J., Yogarajah, M., et al., 2012. Imaging language networks before and after anterior temporal lobe resection: results of a longitudinal fMRI study. Epilepsia 53, 639–650 (Apr).

Protzner, A.B., McAndrews, M.P., 2011. Network alterations supporting word retrieval in patients with medial temporal lobe epilepsy. Journal of Cognitive Neuroscience 23, 2605–2619 (Sep).

Vlooswijk, M.C., Jansen, J.F., Majoie, H.J., et al., 2010. Functional connectivity and language impairment in cryptogenic localization-related epilepsy. Neurology 75, 395–402 (Aug 3).

Luo, C., Qiu, C., Guo, Z., et al., 2011. Disrupted functional brain connectivity in partial epilepsy: a resting-state fMRI study. PLoS One 7, e28196.

Bettus, G., Guedj, E., Joyeux, F., et al., 2009b. Decreased basal fMRI functional connectivity in epileptogenic networks and contralateral compensatory mechanisms. Human Brain Mapping 30, 1580–1591 (May).

Vlooswijk, M.C., Jansen, J.F., Jeukens, C.R., et al., 2011. Memory processes and prefrontal network dysfunction in cryptogenic epilepsy. Epilepsia 52, 1467–1475 (Aug).

van DE, Douw L., Baayen, J.C., et al., 2009. Long-term effects of temporal lobe epilepsy on local neural networks: a graph theoretical analysis of corticography recordings. PLoS One 4, e8081.

Woermann, F.G., Barker, G.J., Birnie, K.D., Meencke, H.J., Duncan, J.S., 1998. Regional changes in hippocampal T2 relaxation and volume: a quantitative magnetic resonance imaging study of hippocampal sclerosis. Journal of Neurology, Neurosurgery, and Psychiatry 65, 656–664 (Nov).

Cook, M.J., Fish, D.R., Shorvon, S.D., Straughan, K., Stevens, J.M., 1992. Hippocampal volumetric and morphometric studies in frontal and temporal lobe epilepsy. Brain 115 (Pt 4), 1001–1015 (Aug).

Lemieux, L., Liu, R.S., Duncan, J.S., 2000. Hippocampal and cerebellar volumetry in serially acquired MRI volume scans. Magnetic Resonance Imaging 18, 1027–1033 (Oct).

Cook, P.A., Symms, M., Boulby, P.A., Alexander, D.C., 2007. Optimal acquisition orders of diffusion-weighted MRI measurements. Journal of Magnetic Resonance Imaging 25, 1051–1058 (May).

Tzourio-Mazoyer, N., Herve, P.Y., Mazoyer, B., 2007. Neuroanatomy: tool for functional localization, key to brain organization. NeuroImage 37, 1059–1060 (Oct 1).

Maldjian, J.A., Laurienti, P.J., Kraft, R.A., Burdette, J.H., 2003. An automated method for neuroanatomic and cytoarchitectonic atlas-based interrogation of fMRI data sets. NeuroImage 19, 1233–1239 (Jul).

Beckmann, C.F., Smith, S.M., 2005. Tensorial extensions of independent component analysis for multisubject FMRI analysis. NeuroImage 25, 294–311 (Mar).

Vollmar, C., O'Muircheartaigh, J., Barker, G.J., et al., 2011. Motor system hyperconnectivity in juvenile myoclonic epilepsy: a cognitive functional magnetic resonance imaging study. Brain 134, 1710–1719 (Jun).

Smith, S.M., Jenkinson, M., Woolrich, M.W., et al., 2004. Advances in functional and structural MR image analysis and implementation as FSL. NeuroImage 23 (Suppl. 1), S208–S219.

Winston, G.P., Daga, P., Stretton, J., et al., 2012. Optic radiation tractography and vision in anterior temporal lobe resection. Annals of Neurology 71, 334–341 (Mar).

Wechsler, D., 1981. Wechsler Adult Intelligence Scale WAIS-R Manual. Rev. ed. Harcourt Brace Jovanovich for The Psychological Corporation, New York.

Canavan, A.G., Passingham, R.E., Marsden, C.D., Quinn, N., Wyke, M., Polkey, C.E., 1989. Sequence ability in parkinsonians, patients with frontal lobe lesions and patients who have undergone unilateral temporal lobectomies. Neuropsychologia 27, 787–798.

Axmacher, N., Mormann, F., Fernandez, G., Cohen, M.X., Elger, C.E., Fell, J., 2007. Sustained neural activity patterns during working memory in the human medial temporal lobe. Journal of Neuroscience 27, 7807–7816 (Jul 18).

Black, L.C., Schefft, B.K., Howe, S.R., Szaflarski, J.P., Yeh, H.S., Privitera, M.D., 2010. The effect of seizures on working memory and executive functioning performance. Epilepsy & Behavior 17, 412–419 (Mar).

Grippo, A., Pelosi, L., Mehta, V., Blumhardt, L.D., 1996. Working memory in temporal lobe epilepsy: an event-related potential study. Electroencephalography and Clinical Neurophysiology 99, 200–213 (Sep).

Krauss, G.L., Summerfield, M., Brandt, J., Breiter, S., Ruchkin, D., 1997b. Mesial temporal spikes interfere with working memory. Neurology 49, 975–980 (Oct).

Wagner, D.D., Sziklas, V., Garver, K.E., Jones-Gotman, M., 2009. Material-specific lateralization of working memory in the medial temporal lobe. Neuropsychologia 47, 112–122 (Jan).

Raichle, M.E., MacLeod, A.M., Snyder, A.Z., Powers, W.J., Gusnard, D.A., Shulman, G.L., 2001. A default mode of brain function. Proceedings of the National Academy of Sciences of the United States of America 98, 676–682 (Jan 16).

Meyer-Lindenberg, A., Poline, J.B., Kohn, P.D., et al., 2001. Evidence for abnormal cortical functional connectivity during working memory in schizophrenia. The American Journal of Psychiatry 158, 1809–1817 (Nov).

Astur, R.S., Constable, R.T., 2004. Hippocampal dampening during a relational memory task. Behavioral Neuroscience 118, 667–675 (Aug).

Astur, R.S., St Germain, S.A., Baker, E.K., Calhoun, V., Pearlson, G.D., Constable, R.T., 2005. fMRI hippocampal activity during a virtual radial arm maze. Applied Psychophysiology and Biofeedback 30, 307–317 (Sep).

Cousijn, H., Rijpkema, M., Qin, S., van Wingen, G.A., Fernandez, G., 2012b. Phasic deactivation of the medial temporal lobe enables working memory processing under stress. NeuroImage 59, 1161–1167 (Jan 16).

Hampson, M., Driesen, N.R., Skudlarski, P., Gore, J.C., Constable, R.T., 2006. Brain connectivity related to working memory performance. Journal of Neuroscience 26, 13338–13343 (Dec 20).

Fair, D.A., Dosenbach, N.U., Church, J.A., et al., 2007. Development of distinct control networks through segregation and integration. Proceedings of the National Academy of Sciences of the United States of America 104, 13507–13512 (Aug 14).

Rudie, J.D., Shehzad, Z., Hernandez, L.M., et al., 2012. Reduced functional integration and segregation of distributed neural systems underlying social and emotional information processing in autism spectrum disorders. Cerebral Cortex 22, 1025–1037 (May).

Janszky, J., Jokeit, H., Heinemann, D., Schulz, R., Woermann, F.G., Ebner, A., 2003. Epileptic activity influences the speech organization in medial temporal lobe epilepsy. Brain 126, 2043–2051 (Sep).

Kaaden, S., Quesada, C.M., Urbach, H., et al., 2011. Neurodevelopmental disruption in early-onset temporal lobe epilepsy: evidence from a voxel-based morphometry study. Epilepsy & Behavior 20, 694–699 (Apr).

Focke, N.K., Yogarajah, M., Bonelli, S.B., Bartlett, P.A., Symms, M.R., Duncan, J.S., 2008. Voxel-based diffusion tensor imaging in patients with mesial temporal lobe epilepsy and hippocampal sclerosis. NeuroImage 40, 728–737 (Apr 1).

Riley, J.D., Franklin, D.L., Choi, V., et al., 2010. Altered white matter integrity in temporal lobe epilepsy: association with cognitive and clinical profiles. Epilepsia 51, 536–545 (Apr).

Keller, S.S., Roberts, N., 2008. Voxel-based morphometry of temporal lobe epilepsy: an introduction and review of the literature. Epilepsia 49, 741–757 (May).

Szaflarski, J.P., Allendorfer, J.B., 2012. Topiramate and its effect on fMRI of language in patients with right or left temporal lobe epilepsy. Epilepsy & Behavior 24, 74–80 (May).

Li, X., Large, C.H., Ricci, R., et al., 2011. Using interleaved transcranial magnetic stimulation/functional magnetic resonance imaging (fMRI) and dynamic causal modeling to understand the discrete circuit specific changes of medications: lamotrigine and valproic acid changes in motor or prefrontal effective connectivity. Psychiatry Research 194, 141–148 (Nov 30).